Electrical Resistivity Tomography (ERT) Laboratory Experiments on Saltwater Encroachment Tracking and Modeling in Saturated Heterogeneous Sediment

Basic Information

Title:	Electrical Resistivity Tomography (ERT) Laboratory Experiments on Saltwater Encroachment Tracking and Modeling in Saturated Heterogeneous Sediment
Project Number:	2008LA57B
Start Date:	3/1/2008
End Date:	2/28/2009
Funding Source:	104B
Congressional District:	6
Research Category:	Ground-water Flow and Transport
Focus Category:	Groundwater, Solute Transport, Methods
Descriptors:	
Principal Investigators:	Frank Tsai

Publication

1. Tsai, F. T.-C. 2009, Saltwater Intrusion Management with Conjunctive Use of Surface Water and Ground Water, Louisiana Water Resources Research Institute, LSU, Baton Rouge, Louisiana, 10
2. Tsai, F. T.-C., and M. Pillala, Subsurface characterization using electrical resistivity tomography, ASCE/EWRI World Water & Environmental Resources Congress, Kansas City, Missouri, May 17-21, 2009.
3. Tsai, F. T.-C., and M. Pillala, Electrical resistivity tomography using MODFLOW, American Geophysical Union 2008 Fall Meeting, San Francisco, CA, Dec 15-19, 2008.

SYNOPSIS

Title: Electrical Resistivity Tomography (ERT) Laboratory Experiments on Saltwater Encroachment Tracking and Modeling in Saturated Heterogeneous Sediment
Project Number:
Start Date: 3/1/2008
End Date: 2/28/2009
Funding Source: 104B
Congressional District: 6
Research Category: Ground-water Flow and Transport
Focus Category: Ground Water, Solute Transport, Methods, Models
Descriptors: Geophysics, Electrical Resistivity, Tomography, MODFLOW, Optimization
Primary PI: Frank T.-C. Tsai

Problem and Research Objectives

Rapid population growth and economic development in southeastern Louisiana have led to increased ground water demand. The East Baton Rouge (EBR) population has been almost doubled since Hurricane Katrina. Moreover, since October 2005, Southern Louisiana has been suffered from the extreme drought. Most of the southern half of the State has averaged just 21 inches of rain, down from the usual 40-inch average. EBR is facing a water demand challenge while experiencing drought. With small to zero expansion of the surface water treatment plants, excessive withdrawal of ground water in the Capital Area is anticipated and will accelerate the existing saltwater encroachment in EBR. Protecting ground water from further saltwater intrusion is an important issue to sustain the economic welfare of the state's citizens.

The goal of this study is to develop an electrical resistivity tomography (ERT) technique to better understand saltwater encroachment in the aquifer. Electrical resistivity tomography (ERT) is a geophysical imaging method which calculates the electrical resistivity distribution in the subsurface environment from a large number of electric potential made from electrodes. ERT has been widely used and successfully explore, monitor subsurface hydrogeological information (USDOE, 2000). ERT is able to determine chloride concentrations in the subsurface (Singha and Gorelick, 2005), flow pathways in the porous media (Daily et al., 1992), and magnitude of hydraulic conductivity (Urish, 1981). ERT was also used as a monitoring tool in the subsurface environmental restoration process to determine the cleanup performance (Ramirez et al., 1993). ERT provides dramatically increased resolution and sensitivity at low cost. Furthermore, ERT is advantageous in characterizing saline tracer at the field site and provides a large number of data with significantly less experiment efforts than those required by the traditional sampling methods (Singha et al., 2003). Moreover, ERT is able to produce two- and three-dimensional images when traditional methods in lab and field measurement allow only limited one-dimensional data.

The objectives of this project include (1) development of ERT experiments, and (2) development of ERT image reconstruction algorithm.

Methodology

(1.1) ERT experiments

This project considers two types of ERT experiments. One is a non-invasive approach through boundary voltage measurement. The other is an invasive approach through measuring voltages at boreholes. The non-invasive approach is shown in Figure 1(a), which measures voltages at electrodes around the boundary of a vessel. The borehole approach is shown in Figure 1(b), which places electrodes along boreholes under the surface. To obtain electric potentials (volts) at electrodes for ERT inversion, given a pair of source electrode and sink electrode (one current pattern), a direct current (DC) power supply injects direct current (amperes) of constant intensity into conductive material to develop an electric potential field. Then, a digital multimeter (DMM) is used to measure voltages (volts) at electrodes with respect to a reference electrode. By assigning zero potential at sink electrode, potentials at all electrodes can be calculated. Numerous electric potential data can be obtained by systematical changing locations of source and sink electrodes (many current patterns) and repeating the measuring protocol.

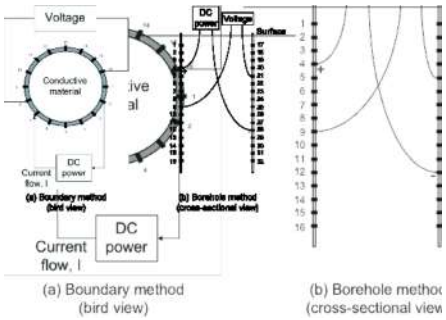

Figure 1: (a) boundary method, and (b) borehole method.

(1.2) ERT devices

A data acquisition (DAQ) system is developed to automatically change locations of source and sink electrodes, take voltage measurements at electrode locations, and record voltages and electric currents to spread sheets. Table 1 lists each device and corresponding function for ERT experiments.

Table 1: Devices for ERT Experiments.

Device	Manufacture	Capacity	Function for ERT	Quan.
EZ Digital GP-1503TP	EZ Digital, Inc.	Max. current output: 3A Max. voltage out: 50V	DC power supply to generate constant voltages or constant currents	1
M9803R	Mastech	Bench-type True RMS Multimeter with RS232 PC interface	DMM for measuring and recording currents	1
NI PCI-4060	National Instruments	5½-digit measurement	DMM for measuring and recording voltages	1
NI SCXI-1127	National Instruments	64-channel multiplexer	1 for switching source electrode locations 1 for switching sink electrode locations 2 for switching electrode locations, where voltages are measured	4
SCXI-1331	National Instruments	64-channel terminal block	Connect wires to SCXI-1127	4
SCXI-1000	National Instruments	4 slots	Chassis for housing multiplexers	3

DMM NI PCI-4060 is installed as an interface card in a personal computer (PC). The PC operation system (OS) is Windows XP Professional Edition. The CPU is Intel Pentium 4 with 3.00GHz. The RAM is 2GB with 2.99GHz. NI LabVIEW8 is used to control the NI devices.

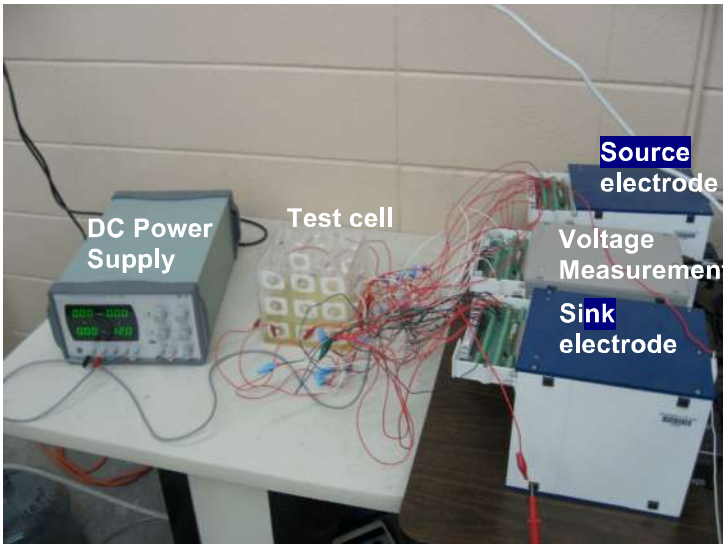

Figure 2: ERT apparatus.

As shown in Figure 2, NI PCI-4060 is connected to one SCXI-1000 chassis (middle) that houses two NI SCXI-1127 switches for measuring voltages. One SCXI-1000 (top) houses one NI SCXI-1127 for changing locations of source electrode. One SCXI-1000 (bottom) houses one NI SCXI-1127 for changing locations of sink electrode. NI LabVIEW8 controls these two switches for sink and sources electrode locations via NI USB-1357 cables.

(1.3) Electric potential modeling (forward problem)

To model electric potential distribution produced by constant DC in a conductive material, this study follows the potential-resistivity differential equation (Vauhkonen et al., 1998), but considers current source term in the governing equation. Let Ω be the domain of conductive material to be imaged and $\partial\Omega$ be the boundary of the domain. The governing equation is

$$\nabla\bullet\left(\rho^{-1}\nabla\phi\right)=I\delta\left(\mathbf{x}-\mathbf{x}_{SO}\right)\quad\text{in }\Omega \tag{1}$$

where ϕ is the electric potential, ρ is the spatially distributed electrical resistivity, I is the constant current, $\mathbf{x}_{SO}$ is the location of source electrode, and δ is the Dirac delta function. The following constraints need to be satisfied

$$\rho^{-1}\frac{\partial\phi}{\partial n}=0\quad\text{on }\partial\Omega\setminus\cup_{\ell=1}^{L}e_{\ell} \tag{2}$$

$$U_{\ell}=\phi+z_{\ell}\rho^{-1}\frac{\partial\phi}{\partial n},\ell=1,2,\cdots L \tag{3}$$

$$I_{\ell}=\int_{e_{\ell}}\rho^{-1}\frac{\partial\phi}{\partial n}dS\quad\text{where }\ell=1,2,\cdots,L \tag{4}$$

where e_ℓ are the electrodes with a surface area S; z_ℓ are the effective contact impedance [ohm-m^2]; U_ℓ are the potentials at electrodes, I_ℓ are the entering or leaving currents through electrodes; and n is the outward normal unit. Eq. (2) represents no potential gradient at the boundary other than at the electrode sites. For electric current conservation, we need to make sure $\sum_{\ell=1}^{L} I_\ell = 0$. Moreover, a zero potential is assigned to the sink electrode.

Equation (1) is identical to the steady-state ground water flow equation with a constant injection rate at source location. Therefore, it is very straightforward for this study to use MODFLOW (Harbaugh et al. 2000) to solve equations (1)-(4). In order to make consistent use of units between the electricity flow and ground water flow, Table 2 lists the analogy of the governing equations and units.

Table 2. Analogy of Electricity Flow and Ground Water Flow

Flow of electricity	Flow of ground water
Ohm's Law: $\bar{J} = -\sigma\nabla\phi = -\rho^{-1}\nabla\phi$ J – current density (ampere/m^2) ρ – electrical resistivity (ohm-m) σ – electrical conductivity (siemen/m) ϕ – electric potential (volt)	Darcy's Law: $\bar{q} = -K\nabla\phi$ q – Darcy's velocity (m/sec) K – hydraulic conductivity (m/sec) ϕ – ground water head (m)
Electric potential equation: $\nabla\bullet\left(\rho^{-1}\nabla\phi\right) = I$ I – electric current (ampere) per material volume	Steady-state ground water flow equation: $\nabla\bullet\left(K\nabla\phi\right) = Q$ Q – volumetric flow rate (m^3/sec) per aquifer volume

(1.4) Effective contact impedance

To model the effective contact impedance in equation (3) in MODFLOW, this study considers the Horizontal Flow Barrier (HFB) Package (Hsieh and Freckleton 1993) and uses the hydraulic characteristic (HC) [1/sec] to mimic the contact impedance. The HC is defined as the barrier hydraulic conductivity divided by the width of the horizontal-flow barrier (Hsieh and Freckleton 1993; Harbaugh, 2005). For a two-dimensional problem, Figure 3 shows the source electrode at one computation cell (source cell). The surface of the source electrode is S_ℓ. The total surface of computation cells (three cells in this figure) with uniform HC surrounding the source cell is $A = A_1 + A_2 + A_3$. Using the concept of equivalent

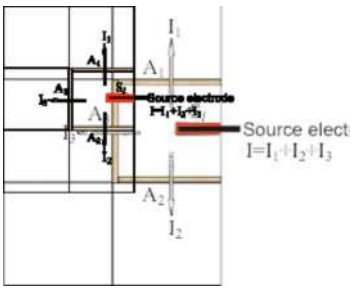

Figure 3: hydraulic characteristic (HC) surrounding the cell of source electrode.

hydraulic conductivity (McDonald and Harbaugh 1988), this study finds the relationship

$$z_\ell = \frac{1}{HC_\ell}\frac{A}{S_\ell} \tag{5}$$

The contact impedance can be calculated once the hydraulic characteristic is obtained.

(2.1) ERT inversion (inverse problem)

Using electric potential data, this study reconstructs the electrical resistivity distribution by minimizing the sum of errors between calculated potentials and measured potentials at electrode locations for all current patterns:

$$\min_{\sigma(\mathbf{x})} \quad E = \sum_{p=1}^{P}\sum_{\ell=1}^{L}\left(\phi_{p,\ell} - \phi_{p,\ell}^{obs}\right)^2 \tag{6}$$

where $\phi_{p,\ell}$ is the calculated potential at electrode ℓ with current pattern p; and $\phi_{p,\ell}^{obs}$ is the measured potential at electrode ℓ with current pattern p. Since electrical conductivity is reciprocal of electrical resistivity, this study estimates electrical conductivity for each computation cells Many studies have suggested regularization terms to ERT inversion (Zhang et al., 1995; Dickin and Wang, 1996; Vauhkonen et al., 1998). This study does not consider regularization.

(2.2) Adjoint-state method

This study adopts an adjoint-state method to calculate the gradients, $\frac{\partial E}{\partial \sigma}$, for a gradient-based optimization method because of its computational efficiency. Using adjoint-state techniques in Sun (1994), one can obtain the adjoint state equation for equation (1) with current pattern p:

$$\nabla\bullet\left(\sigma\nabla\psi_p\right) = -2\sum_{\ell=1}^{L}\left(\phi_{p,\ell} - \phi_{p,\ell}^{obs}\right)\delta\left(\mathbf{x} - \mathbf{x}_{p,\ell}\right) \tag{7}$$

where ψ_p is the adjoint state variable for current pattern p. The boundary condition is $\sigma\nabla\psi_p\bullet\bar{n} = 0$. Moreover, $\psi_p = 0$ is assigned to the sink electrode.

Equation (7) is mathematically identical to equation (1) and can be solved by MODFLOW. One just needs to replace the single source term in equation (1) with 2 times misfit error in equation (7) at each electrode location. Then, the gradients are

$$\frac{\partial E}{\partial \sigma_j} = \sum_{p=1}^{P}\int_{\Omega_j}\left[\nabla\psi_p\bullet\nabla\phi_p\right]d\Omega \tag{8}$$

where Ω_j is the influence domain of unknown σ_j.

For a total of P current patterns, one needs to execute $2P$ runs of MODFLOW in order to calculate all gradients for one optimization iteration.

Principal Findings and Significance

Case 1: Estimating contact impedance of electrodes

The first case is to estimate HC values for contact impedance of electrodes via the boundary method. Figure 4(a) shows a test cell with three layers of electrodes. The electrodes were made of stainless steel screws (18-8 SS Cup Point Socket Set Screw, 10-24 Thread, 1 in. long) from McMASTER-CARR. Each layer contains 12 electrodes. The dimension of the test cell is 6 in. by 6 in. by 6 in. The spacing between electrodes at each side of the box is 2 in. The spacing between the electrodes of the bottom layer and the bottom of the test cell is 1 in. For a two-dimensional ERT experiment, a 2 in. of tap water in depth is considered in the test cell, which submerged the electrodes of the bottom layer. The electrical conductivity of tap water is 0.042 S/m, measured by Extech EC400 Conductivity/TDS/Salinity Meter.

For the ERT data, 12 electrodes give the maximum of 132 ($=12\times11$) current patterns. Figure 4(b) represents 11 current patterns, where source electrode stays at #1 while sink electrode is moving from #2 to #12. Each pattern has constant DC of 5 mA. A total of 1452 potential data are obtained. This case considers an unknown conductivity for homogeneous tap water and 12 unknown HC values for 12 electrodes. Therefore, there are 13 unknown values needed to be estimated.

For ERT inversion, the model domain was discretized into 37 by 37 square computation cells. The thickness of the model domain is 2 in. Figure 4(c) shows the model discretization and the location of electrodes. We adopted a BFGS (Broyden-Fletcher-Goldfarb-Shanno) solver (Byrd et al., 1994), a quasi-Newton method, to solve equation (6). The estimated electrical conductivity is 0.045 S/m. The estimated HC values varied from 1.4 to 2.3 sec^{-1}.

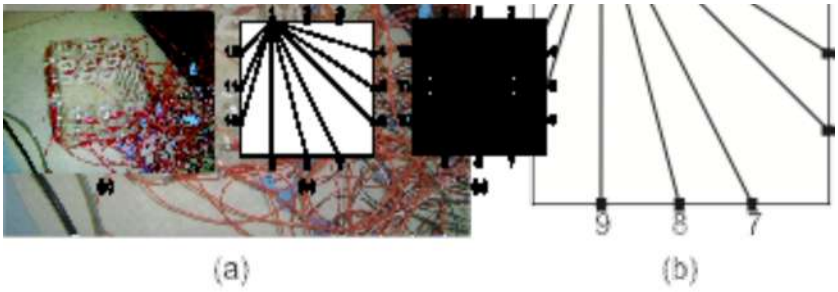

Figure 4: (a) test cell, (b) 11 current patterns (source electrode at #1 and sink electrode moves from #2 to #12), and (c) domain discretization.

Case 2: Two-dimensional numerical study

To better understand the capability of estimating electrical conductivity for each computation cell, this case conducted a numerical experiment using the same settings in the first case. Figure

5(a) shows the true conductivity field, where a high conductive zone (0.95 S/m) is inside a low conductive area (0.05 S/m). Again, the domain is discretized into 37 by 37 computation cells. Therefore, there are 1369 unknowns. With 132 currents, there are 1452 potential data. The HC valued identified in the first case was used. Figure 5(b) shows the estimated conductivity distribution. Figure 5(c) shows the decreasing fitting error over the number of called objective functions. Even though the fitting error is small, the estimated conductivity field is not close to the true solution. However the location of relative high conductivity zone indicates the capability of the ERT inverse technique. The poor result is due to the ill-posted inverse problem in this case, where the number of unknowns is very close to the number of data. This indicates an over parameterization problem.

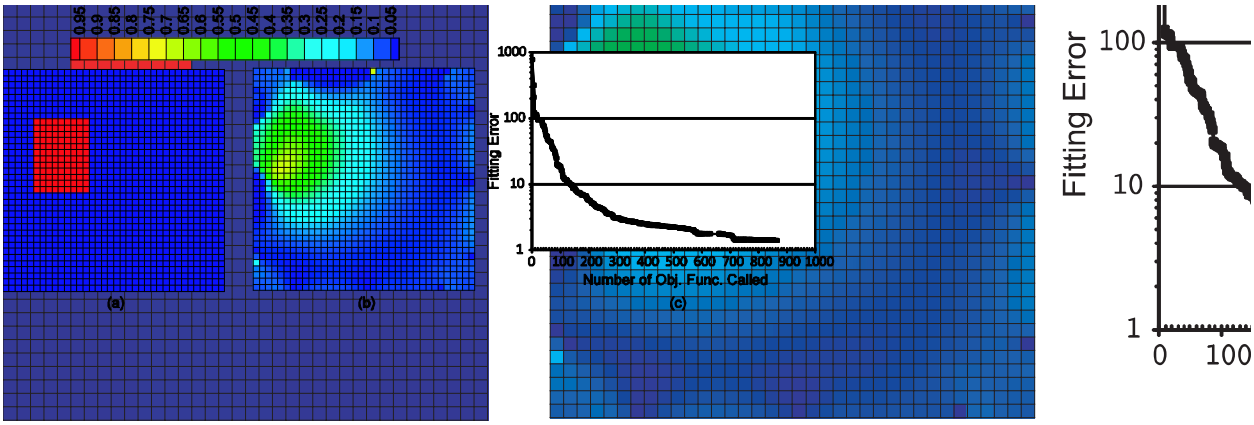

Figure 5: (a) true conductivity (S/m) distribution, (b) estimated conductivity distribution, and (c) fitting error.

Case 3: Numerical study on borehole approach

To ensure a good ERT image for the borehole approach, this case considers a numerical study on a two-dimensional field with a dimension of 50 cm wide by 100 cm deep. The true conductivity field is shown in Figure 6(a), where a square block with 0.95 S/m and a rectangular block with 0.15 S/m are inside a background material with 0.05 S/m.

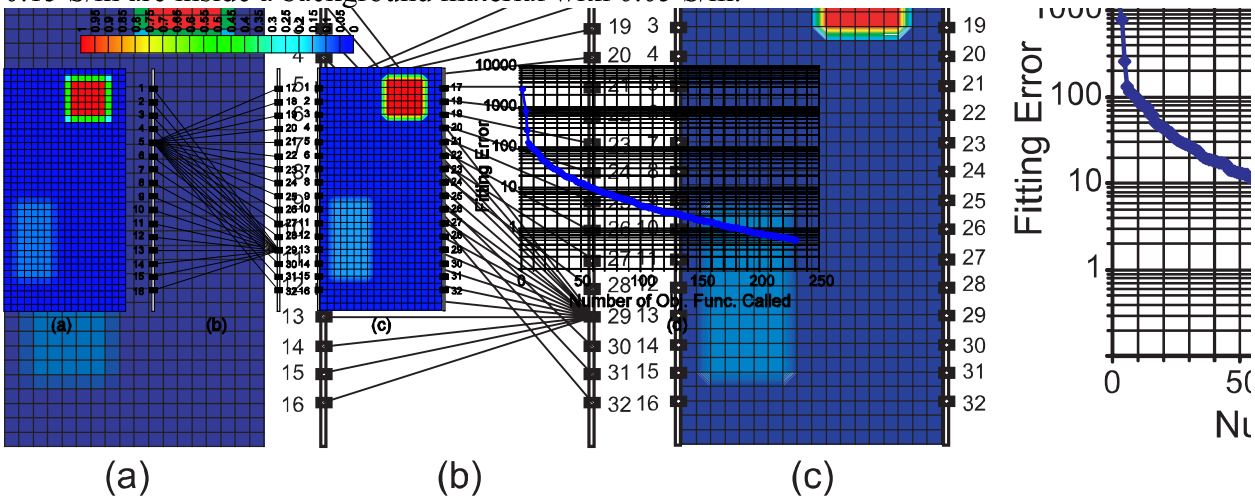

Figure 6: (a) true conductivity field (S/m), (b) source electrode at #5 and sink electrode moving from #17 to #32 and source electrode at #29 and sink electrode moving from #1 to #16, (c) estimated conductivity field, and (d) fitting error.
Two boreholes shown in Figure 6(b) are designed such that each borehole has 16 electrodes. The spacing between electrodes in each borehole is 5 cm. This case considered 512 ($= 32 \times 16$) current patterns. Constant DC of 2 mA was applied. Therefore, a total of 15872 potential data are obtained.

For ERT inversion, the domain was discretized into 37 by 19 computation cells. Unknown conductivity values for 703 computation cells were estimated by 15872 potential data. Clearly, Figure 6(c) shows a good ERT image. Figure 6(d) shows the fitting error minimization process.

Case 4 ERT using borehole approach
With the same settings in Case 3, the ERT technique was applied to a sand tank fill with sand and tap water. The dimension of the sand tank is 100 cm by 100 cm by 5 cm. Two reservoirs are at right and left sides (See Figure 7(a)). The sand has a uniform coefficient of 1.8. The grain size d_{50} is 0.45 mm. The porosity is 0.4. A falling head test was conducted to obtain saturated hydraulic conductivity to be 20.35 m/day.

A block of wood is buried inside the sand tank between two boreholes of electrodes, whose spacing is 50 cm. Their locations are shown in Figure 7(a). Using the same inverse technique in Case 3, Figure 7(b) shows a good ERT image, which locates the wood block.

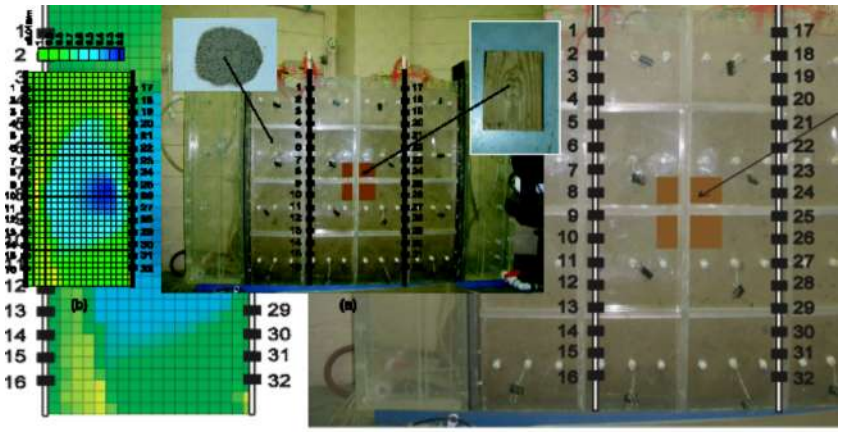

(b) (a)

Figure 7: (a) sand tank, and (b) ERT image.

Summary

[1] This project has demonstrated the ERT to be a potential geophysical technique to monitor subsurface environment. ERT is low cost and produces abundant data for the inverse problem.
[2] This project has extended MODFLOW applicability to solve the potential-resistivity model for ERT applications. Particularly, this study utilizes the hydraulic characteristic in the Horizontal Flow Barrier (HFB) Package to represent effective contact impedance of electrodes.
[3] The ERT inversion is conducted by a simulation-optimization approach that links MODFLOW with a BFGS optimization solver. The adjoint state method presents an efficient method to obtain gradient for each computation grid.
[4] The quality of ERT images depends on many factors, including the quality and quantity of measured voltages, the considered resolution of resistivity, the current patterns, the electrode locations. The most challenge task is the interpretation of electrical resistivity to hydraulic property. These issues require further extensive study.

References

Byrd, R.H., P. Lu, J. Nocedal, and C. Zhu. (1994). A limited memory algorithms for bound constrained optimization. Northwestern University, Department of Electrical Engineering and Computer Science, Technical Report NAM-08.

Dickin, F., and M. Wang. (1996). Electrical resistance tomography for process applications. Measurement Science & Technology 7(3), 247-260.

Harbaugh, A. W., E. R. Banta, M. C. Hill, and M. G. McDonald. (2000). MODFLOW-2000, the U.S. Geological Survey modular ground-water model -- User guide to modularization concepts and the Ground-Water Flow Process. U.S. Geological Survey Open-File Report 00-92.

Harbaugh, A. W. (2005). MODFLOW-2005, the U.S. Geological Survey modular ground-water model: the Ground-Water Flow Process, U.S.G.S. Techniques and Methods 6-A16.

McDonald, M.G., and A.W. Harbaugh. (1988). A modular three-dimensional finite-difference ground-water flow model: U.S. Geological Survey Techniques of Water-Resources Investigations, book 6, chap. A1, 586 p.

Hsieh, P. A., and J. R. Freckleton. (1993). Documentation of a computer program to simulate horizontal-flow barriers using the U.S. Geological Survey's Modular Three-Dimensional Finite-Difference Ground-Water flow model, U.S.G.S., Open-File Report 92-477.

Ramirez, A., W. Daily, D. Labrecque, E. Owen, and D. Chesnut. (1993). Monitoring an underground steam injection process using electrical-resistance tomography. Water Resources Research 29(1), 73-87.

Singha, K., A. M. Binley, J. W. Lane, Jr.,, and S. M. Gorelick. (2003). Electrical imaging of tracer migration at the Massachusetts Military Reservation, Cape Code. In Symposium on the Application of Geophysics to Engineering and Environmental Problems (SAGEEP), April 6-10, 2003, San Antonio, Texas, Proceedings: Denver, Colorado, Environmental and Engineering Geophysical Society, CD-ROM, 11p.

Singha, K., and S. M. Gorelick. (2005). Saline tracer visualized with three-dimensional electrical resistivity tomography: Field-scale spatial moment analysis. Water Resources Research 41(5).

Urish, D. W. (1981). Electrical resistivity-hydraulic conductivity relationships in glacial outwash aquifers. Water Resources Research 17(5), 1401-1408.

USDOE. (2000). Electrical Resistance Tomography for Subsurface Imaging. Summary Report, DOE/EM-0538.

Vauhkonen, M., D. Vadasz, P. A. Karjalainen, E. Somersalo, and J. P. Kaipio. (1998). Tikhonov regularization and prior information in electrical impedance tomography. IEEE Transactions on Medical Imaging 17(2), 285-293.

Zhang, J., R. L. Mackie, and T. R. Madden. (1995). 3-D resistivity forward modeling and inversion using conjugate gradients. Geophysics 60(5), 1313-1325.